J Low Temp Phys (2016) 185:508–514
DOI 10.1007/s10909-015-1427-2

Effect of the Long-Range Coulomb Interaction on the Phase Diagram of the Kohn–Luttinger Superconducting State in Idealized Graphene

M. Yu. Kagan[1,2] · V. A. Mitskan[3,4] · M. M. Korovushkin[3]

Received: 8 June 2015 / Accepted: 8 December 2015 / Published online: 29 December 2015

Abstract The effect of the long-range Coulomb interaction on the formation of the Kohn–Luttinger superconductivity in monolayer doped graphene is studied disregarding the Van der Waals potential of the substrate and both magnetic and non-magnetic impurities. It is shown that the allowance for the Kohn–Luttinger renormalizations up to the second order in perturbation theory in the on-site Hubbard interaction inclusively, as well as in the intersite Coulomb interaction, significantly affects the interplay between the superconducting phases with the f-wave, $p+ip$-wave, and $d+id$-wave symmetries of the order parameter. It is demonstrated that taking Coulomb repulsion of electrons located at the next-nearest neighboring atoms in such a system into account changes qualitatively the phase diagram and enhances the critical temperature of the transition to the superconducting phase.

Keywords Unconventional superconductivity · Kohn–Luttinger mechanism · Graphene monolayer

✉ M. M. Korovushkin
kmax@iph.krasn.ru

M. Yu. Kagan
kagan@kapitza.ras.ru

1 P. L. Kapitza Institute for Physical Problems, Russian Academy of Sciences, Moscow, Russia 119334

2 National Research University Higher School of Economics, Moscow, Russia 109028

3 L. V. Kirensky Institute of Physics, Siberian Branch of Russian Academy of Sciences, Krasnoyarsk, Russia 660036

4 M. F. Reshetnev Siberian State Aerospace University, Krasnoyarsk, Russia 660014

1 Introduction

At the present time, the possible development of superconductivity in the framework of the Kohn–Luttinger mechanism [1], suggesting the emergence of superconducting pairing in the systems with purely repulsive interaction [2], in graphene under appropriate experimental conditions is widely discussed. Despite the fact that intrinsic superconductivity so far has not been observed in graphene, the stability of the Kohn–Luttinger superconducting phase has been investigated and the symmetry of the order parameter in the hexagonal lattice was identified. It was found [3] that chiral superconductivity [4] with the $d + id$-wave symmetry of the order parameter prevails in a large domain near the Van Hove singularity in the density of states (DOS). The competition between the superconducting phases with different symmetry types in the wide electron density range $1 < n \leq n_{\mathrm{VH}}$, where n_{VH} is the Van Hove filling, in the graphene monolayer was studied in papers [5,6]. It was demonstrated that at intermediate electron densities the Coulomb interaction of electrons located on the nearest carbon atoms facilitates implementation of superconductivity with the f-wave symmetry of the order parameter, while at approaching the Van Hove singularity, the superconducting $d + id$-wave pairing evolves [5,6].

In this work, we investigate the role of the Coulomb repulsion of electrons located at the next-nearest neighboring carbon atoms in the development of the Kohn–Luttinger superconductivity in an idealized graphene monolayer disregarding the effect of the Van der Waals potential of the substrate and both magnetic and non-magnetic impurities. Using the Shubin–Vonsovsky (extended Hubbard) model in the Born weak-coupling approximation, we construct the phase diagram determining the boundaries of superconducting regions with different types of the symmetry of the order parameter. It is shown that taking Coulomb repulsion of electrons located at the next-nearest neighboring sites of hexagonal lattice into account leads to a qualitative modification of the phase diagram, as well as to an increase in the critical temperature of the transition to the superconducting state in the system.

2 Theoretical Model

In the hexagonal lattice of graphene, each unit cell contains two carbon atoms; therefore, the entire lattice can be divided into two sublattices A and B. In the Shubin–Vonsovsky model [7], the Hamiltonian for the graphene monolayer taking into account electron hoppings between the nearest atoms, as well as the Coulomb repulsion between electrons located at one, neighboring and next-nearest neighboring atoms in the Wannier representation, has the form:

$$\hat{H} = \hat{H}_0 + \hat{H}_{\mathrm{int}}, \tag{1}$$

$$\hat{H}_0 = -\mu \left(\sum_{f\sigma} \hat{n}^A_{f\sigma} + \sum_{g\sigma} \hat{n}^B_{g\sigma} \right) - t_1 \sum_{f\delta\sigma} \left(a^\dagger_{f\sigma} b_{f+\delta,\sigma} + \mathrm{h.c.} \right),$$

$$\hat{H}_{\rm int} = U\left(\sum_f \hat{n}^A_{f\uparrow}\hat{n}^A_{f\downarrow} + \sum_g \hat{n}^B_{g\uparrow}\hat{n}^B_{g\downarrow}\right) + V_1 \sum_{f\delta\sigma\sigma'} \hat{n}^A_{f\sigma}\hat{n}^B_{f+\delta,\sigma'} + \frac{V_2}{2}\left(\sum_{\langle\langle fm\rangle\rangle\sigma\sigma'} \hat{n}^A_{f\sigma}\hat{n}^A_{m\sigma'} + \sum_{\langle\langle gr\rangle\rangle\sigma\sigma'} \hat{n}^B_{g\sigma}\hat{n}^B_{r\sigma'}\right).$$

Here, operators $a^\dagger_{f\sigma}(a_{f\sigma})$ create (annihilate) an electron with spin projection $\sigma = \pm 1/2$ at the site f of the sublattice A; $\hat{n}^A_{f\sigma} = a^\dagger_{f\sigma}a_{f\sigma}$ denotes the operator of the number of fermions at the f site of the sublattice A (analogous notation is used for the sublattice B). Vector δ connects the nearest atoms of the hexagonal lattice. We assume that the position of the chemical potential μ and the number of carriers n in the graphene monolayer can be controlled by a gate electric field. In the Hamiltonian, t_1 is the hopping integral between the neighboring atoms (hoppings between different sublattices), U is the parameter of Hubbard repulsion between electrons of the same site with the opposite spin projections, and V_1 and V_2 are the Coulomb interactions between electrons of the neighboring and the next-nearest neighboring carbon atoms in the monolayer. In the Hamiltonian, the symbol $\langle\langle\ \rangle\rangle$ indicates that the summation is carried out only over the next-nearest neighbors.

Proceeding to the momentum space and performing the Bogoliubov transformation,

$$\alpha_{i\mathbf{k}\sigma} = w_{i1}(\mathbf{k})a_{\mathbf{k}\sigma} + w_{i2}(\mathbf{k})b_{\mathbf{k}\sigma}, \qquad i = 1, 2, \tag{2}$$

we diagonalize Hamiltonian $\hat{H}_0$, which acquires the form:

$$\hat{H}_0 = \sum_{i=1}^{2}\sum_{\mathbf{k}\sigma} E_{i\mathbf{k}}\alpha^\dagger_{i\mathbf{k}\sigma}\alpha_{i\mathbf{k}\sigma}. \tag{3}$$

The two-band energy spectrum is described by the expressions [8]

$$E_{1\mathbf{k}} = t_1|u_{\mathbf{k}}| - t_2 f_{\mathbf{k}}, \qquad E_{2\mathbf{k}} = -t_1|u_{\mathbf{k}}| - t_2 f_{\mathbf{k}}, \tag{4}$$

where the following notation has been introduced:

$$f_{\mathbf{k}} = 2\cos(\sqrt{3}k_y a) + 4\cos\left(\frac{\sqrt{3}}{2}k_y a\right)\cos\left(\frac{3}{2}k_x a\right),$$
$$u_{\mathbf{k}} = \sum_\delta e^{i\mathbf{k}\delta} = e^{-ik_x a} + 2e^{\frac{i}{2}k_x a}\cos\left(\frac{\sqrt{3}}{2}k_y a\right), \qquad |u_{\mathbf{k}}| = \sqrt{3 + f_{\mathbf{k}}}.$$

In this paper, we use the Born weak-coupling approximation, in which the hierarchy of model parameters has the form:

$$W > U > V_1 > V_2, \tag{5}$$

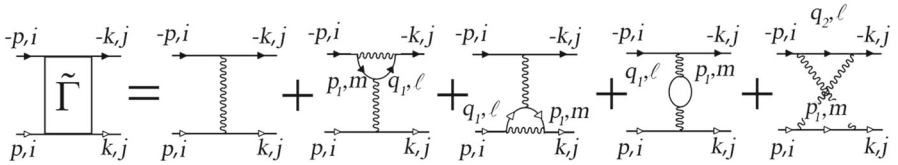

Fig. 1 First- and second-order diagrams for the effective interaction of electrons in the graphene monolayer. *Solid lines with light* (*dark*) *arrows* correspond to the Green functions for electrons with spin projections $+\frac{1}{2}$ $(-\frac{1}{2})$ and energies corresponding to graphene energy bands E_i and E_j. Subscripts i and j can acquire the values of 1 or 2. Here momenta $\mathbf{q}_1 = \mathbf{p}_1 + \mathbf{p} - \mathbf{k}$ and $\mathbf{q}_2 = \mathbf{p}_1 - \mathbf{p} - \mathbf{k}$ are introduced

where W is the bandwidth in the graphene monolayer (4). In the calculation of the scattering amplitude in the Cooper channel, the condition (5) allows us to limit the consideration only to the second-order diagrams in the effective interaction of two electrons with the opposite values of the momentum and spin and to use the quantity $\widetilde{\Gamma}(\mathbf{p}, \mathbf{k})$ for it. Graphically, this quantity is determined by the sum of the diagrams shown in Fig. 1. It is well known that the possibility of Cooper pairing is determined by the characteristics of the energy spectrum near the Fermi level and by the effective interaction of electrons located near the Fermi surface [9]. Assuming that the chemical potential in doped monolayer graphene falls into the upper energy band $E_{1\mathbf{k}}$ and analyzing the conditions for the occurrence of the Kohn–Luttinger superconductivity, we can consider the situation in which the initial and final momenta of electrons in the Cooper channel also belong to the upper band. In this paper, we perform the calculation of the phase diagram of the superconducting state in graphene following the scheme we used in our previous work [5].

3 Results

Figure 2a shows the calculated phase diagram of the superconducting state in a graphene monolayer as a function of the carrier concentration n and V_1 for the set of parameters $U = 2|t_1|$, and the Coulomb interaction $V_2 = 0$. It can be seen that the phase diagram consists of three regions. At low electron densities n, the ground state of the system corresponds to the chiral superconductivity with the $d + id$-wave symmetry of the order parameter [4]. At intermediate electron densities, the superconducting f-wave pairing is implemented. At the large values of n, the domain of the superconducting $d + id$-wave pairing occurs [3]. With the increase of the parameter V_1 of the intersite Coulomb interaction, in the region of small values of n, the $d + id$-wave pairing is suppressed and the pairing with the f-wave symmetry of the order parameter is implemented. Thin blue lines in Fig. 2 are the lines of equal values of the effective coupling constant $|\lambda|$. It can be seen that in this case in the vicinity of n_{VH} the effective coupling constant reaches the value of $|\lambda| = 0.1$.

It should be noted that to avoid the summation of the parquet diagrams [10,11], we do not analyze here the electron density regions that are very close to n_{VH}. For this reason, the boundaries between different domains of the implementation of the superconducting pairing, as well as the lines of the equal value of $|\lambda|$ that are very close to the Van Hove singularity, are indicated in the phase diagram by dashed lines.

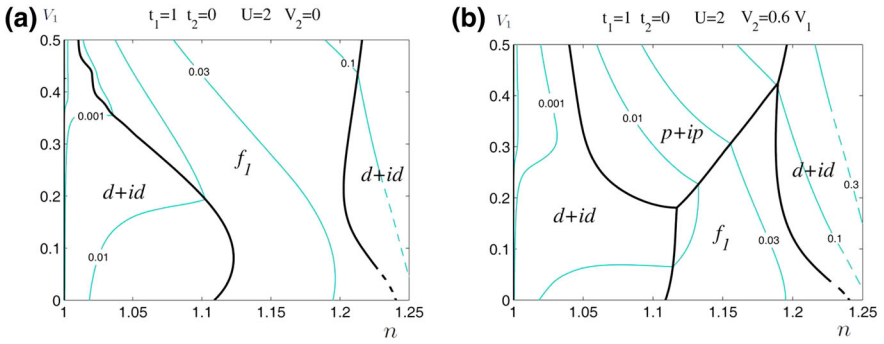

Fig. 2 Phase diagram of the superconducting state of the graphene monolayer shown as a function of the variables "$n - V_1$" at $U = 2|t_1|$ for **a** $V_2 = 0$ and **b** $V_2 = 0.6V_1$. For all the points on the same *thin blue line*, the value of $|\lambda|$ is constant and marked with the corresponding number (Color figure online)

Let us consider the modification of the phase diagram for the graphene monolayer with regard to the Coulomb interaction V_2 between the electrons located at the next-nearest carbon atoms. It can be seen from Fig. 2b for the fixed ratio between the parameters of the long-range Coulomb interactions $V_2 = 0.6V_1$ that when V_2 is taken into account, the phase diagram changes qualitatively. This evolution involves the suppression of a large region of the superconducting state with the f-wave symmetry at the intermediate electron densities and the implementation of the chiral superconducting pairing with the $p + ip$-wave symmetry of the order parameter. In addition, when V_2 is taken into account, the effective coupling constant increases to the value of $|\lambda| = 0.3$. Consequently, it leads to a significant increase in critical temperatures of the superconducting transitions in idealized doped graphene. Note that here we do not take electron hoppings to the next-nearest carbon atoms t_2 into account, because switching on of these hoppings for the graphene monolayer does not significantly

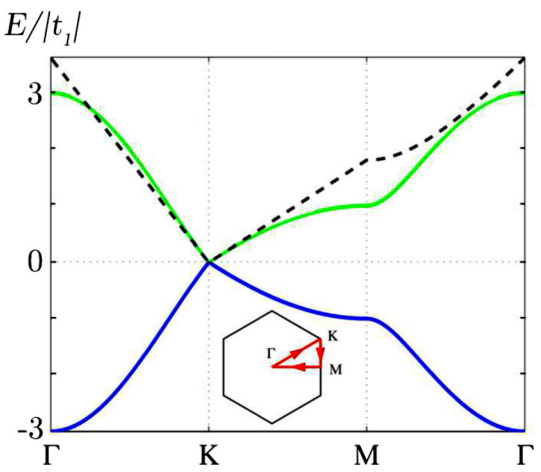

Fig. 3 Energy spectra of a graphene monolayer defined by (4) (*blue* and *green solid lines*) and energy spectra obtained in the framework of the Dirac approximation (*black dashed line*). Subplot depicts the path around the Brillouin zone (Color figure online)

6. R. Nandkishore, R. Thomale, A.V. Chubukov, Phys. Rev. B **89**, 144501 (2014)
7. S. Shubin, S. Vonsovsky, Proc. R. Soc. A **145**, 159 (1934)
8. P.R. Wallace, Phys. Rev. **71**, 622 (1947)
9. L.P. Gor'kov, T.K. Melik-Barkhudarov, JETP **13**, 1018 (1961)
10. I.E. Dzyaloshinskii, V.M. Yakovenko, JETP **67**, 844 (1988)
11. I.E. Dzyaloshinskii, I.M. Krichever, Ya. Khronek, JETP **67**, 1492 (1988)
12. A.I. Posazhennikova, M.V. Sadovskii, JETP Lett. **63**, 358 (1996)